



CERN-EP-2017-241
12 September 2017

Constraining the magnitude of the Chiral Magnetic Effect with Event Shape Engineering in Pb–Pb collisions at $\sqrt{s_{\text{NN}}} = 2.76$ TeV

ALICE Collaboration

Abstract

In ultrarelativistic heavy-ion collisions, the event-by-event variation of the elliptic flow v_2 reflects fluctuations in the shape of the initial state of the system. This allows to select events with the same centrality but different initial geometry. This selection technique, Event Shape Engineering, has been used in the analysis of charge-dependent two- and three-particle correlations in Pb–Pb collisions at $\sqrt{s_{\text{NN}}} = 2.76$ TeV. The two-particle correlator $\langle \cos(\varphi_\alpha - \varphi_\beta) \rangle$, calculated for different combinations of charges α and β , is almost independent of v_2 (for a given centrality), while the three-particle correlator $\langle \cos(\varphi_\alpha + \varphi_\beta - 2\Psi_2) \rangle$ scales almost linearly both with the event v_2 and charged-particle pseudorapidity density. The charge dependence of the three-particle correlator is often interpreted as evidence for the Chiral Magnetic Effect (CME), a parity violating effect of the strong interaction. However, its measured dependence on v_2 points to a large non-CME contribution to the correlator. Comparing the results with Monte Carlo calculations including a magnetic field due to the spectators, the upper limit of the CME signal contribution to the three-particle correlator in the 10–50% centrality interval is found to be 26–33% at 95% confidence level.

arXiv:1709.04723v1 [nucl-ex] 14 Sep 2017

Parity symmetry is conserved in electromagnetism and is maximally violated in weak interactions. In strong interactions, global parity violation is not observed even though it is allowed by quantum chromodynamics. Local parity violation in strong interactions might occur in microscopic domains under conditions of finite temperature [1–4] due to the existence of the topologically non-trivial configurations of the gluonic field, instantons and sphalerons. The interactions between quarks and gluonic fields with non-zero topological charge [5] change the quark chirality. A local imbalance of chirality, coupled with the strong magnetic field produced in heavy-ion collisions ($B \sim 10^{15}$ T) [6–8], would lead to charge separation along the direction of the magnetic field, which is on average perpendicular to the reaction plane (the plane of symmetry defined by the impact parameter vector and the beam direction), a phenomenon called Chiral Magnetic Effect (CME) [9–12]. Since the sign of the topological charge is equally probable to be positive or negative, the charge separation averaged over many events is zero. This makes the observation of the CME experimentally difficult and possible only via correlation techniques.

Azimuthal anisotropies in particle production relative to the reaction plane, often referred to as anisotropic flow, are an important observable to study the system created in heavy-ion collisions [13, 14]. Anisotropic flow arises from the asymmetry in the initial geometry of the collision. Its magnitude is quantified via the coefficients v_n in a Fourier decomposition of the charged particle azimuthal distribution [15, 16]. Local parity violation would result in an additional sine term [17]

$$\frac{dN}{d\Delta\varphi_\alpha} \sim 1 + 2v_{1,\alpha} \cos(\Delta\varphi_\alpha) + 2a_{1,\alpha} \sin(\Delta\varphi_\alpha) + 2v_{2,\alpha} \cos(2\Delta\varphi_\alpha) + \dots, \quad (1)$$

where $\Delta\varphi_\alpha = \varphi_\alpha - \Psi_{\text{RP}}$, φ_α is the azimuthal angle of the particle of charge α (+, -) and Ψ_{RP} is the reaction-plane angle. The first ($v_{1,\alpha}$) and the second ($v_{2,\alpha}$) coefficients are called directed and elliptic flow, respectively. The $a_{1,\alpha}$ coefficient quantifies the effects from local parity violation. Since the average $\langle a_{1,\alpha} \rangle = 0$ over many events, one can only measure $\langle a_{1,\alpha}^2 \rangle$ or $\langle a_{1,+} a_{1,-} \rangle$. The charge-dependent two-particle correlator

$$\delta_{\alpha\beta} \equiv \langle \cos(\varphi_\alpha - \varphi_\beta) \rangle = \langle \cos(\Delta\varphi_\alpha) \cos(\Delta\varphi_\beta) \rangle + \langle \sin(\Delta\varphi_\alpha) \sin(\Delta\varphi_\beta) \rangle \quad (2)$$

is not convenient for such a study, because along with the signal $\langle a_{1,\alpha} a_{1,\beta} \rangle$ (β denotes the charge) there is a much stronger contribution from correlations unrelated to the azimuthal asymmetry in the initial geometry (“non-flow”). These correlations largely come from the inter-jet correlations and resonance decays. To increase the CME contribution it was proposed to use the following correlator [17]

$$\gamma_{\alpha\beta} \equiv \langle \cos(\varphi_\alpha + \varphi_\beta - 2\Psi_{\text{RP}}) \rangle = \langle \cos(\Delta\varphi_\alpha) \cos(\Delta\varphi_\beta) \rangle - \langle \sin(\Delta\varphi_\alpha) \sin(\Delta\varphi_\beta) \rangle \quad (3)$$

that measures the difference between the correlation projected onto the reaction plane and perpendicular to it. In practice, the reaction-plane angle is estimated by constructing the event plane angle Ψ_2 using azimuthal particle distributions, which is why this correlator is often described as a three-particle correlator. This correlator suppresses background contributions at the level of v_2 , the difference between the particle production in-plane and out-of-plane. Examples of such background sources are the local charge conservation (LCC) coupled with elliptic flow [18, 19], momentum conservation [19–21], and directed-flow fluctuations [22]. The most significant background source for CME measurements is the LCC.

The measurements of charge-dependent azimuthal correlations performed at the Relativistic Heavy Ion Collider (RHIC) [23–26] are in qualitative agreement with the expectations for the CME. The ALICE measurements at the Large Hadron Collider (LHC) [27, 28] also do not allow for a firm conclusion about the CME signal at the LHC energies because the interpretation of the results is complicated due to possible background contributions. The Event Shape Engineering (ESE) technique was proposed to disentangle background contributions from the potential CME signal [29]. This method makes it possible to select events with eccentricity values significantly larger or smaller than the average in a given centrality

class [30, 31] since v_2 scales approximately linearly with eccentricity [32]. The CME contribution is expected to mainly scale with the magnetic field strength and to not have a strong dependence on the eccentricity [33], while the background varies significantly. Therefore ESE provides a unique tool to separate the CME signal from the background for the three-particle correlator.

The CMS Collaboration has recently reported the measurement of the three-particle correlator $\gamma_{\alpha\beta}$ in p–Pb collisions at $\sqrt{s_{\text{NN}}} = 5.02$ TeV [34], where the direction of the magnetic field is expected to be uncorrelated to the reaction plane [35]. The magnitude of the correlator in p–Pb and Pb–Pb collisions is comparable for similar final-state charged-particle multiplicities. This measurement indicates that the contribution of the CME to this observable in this multiplicity range is small.

In this paper we report the measurements of the two-particle correlator $\delta_{\alpha\beta}$, the three-particle correlator $\gamma_{\alpha\beta}$, and the elliptic flow v_2 of unidentified charged particles. These measurements are performed for shape selected and unbiased events in Pb–Pb collisions at $\sqrt{s_{\text{NN}}} = 2.76$ TeV. An upper limit on the CME contribution is deduced from comparisons of the observed dependence of the correlations on the event v_2 to that estimated using Monte Carlo (MC) simulations of the magnetic field of spectators with different initial conditions. While this paper was in preparation, a paper employing a similar approach to estimate the fraction of the CME signal in the three-particle correlator was submitted by the CMS Collaboration [36].

The data sample recorded by ALICE during the 2010 LHC Pb–Pb run at $\sqrt{s_{\text{NN}}} = 2.76$ TeV is used for this analysis. General information on the ALICE detector and its performance can be found in [37, 38]. The Time Projection Chamber (TPC) [37, 39] and Inner Tracking System (ITS) [37, 40] are used to reconstruct charged-particle tracks and measure their momenta with a track-momentum resolution better than 2% for the transverse momentum interval $0.2 < p_{\text{T}} < 5.0$ GeV/c [38]. The two innermost layers of the ITS, the Silicon Pixel Detector (SPD), are employed for triggering and event selection. Two scintillator arrays (V0) [37, 41], which cover the pseudorapidity ranges $-3.7 < \eta < -1.7$ (V0C) and $2.8 < \eta < 5.1$ (V0A), are used for triggering, event selection, and the determination of centrality [42] and Ψ_2 . The trigger conditions and the event selection criteria are described in [38]. An offline event selection is applied to remove beam induced background and pileup events. Approximately $9.8 \cdot 10^6$ minimum-bias Pb–Pb events with a reconstructed primary vertex within ± 10 cm from the nominal interaction point in the beam direction are in 0–60% centrality interval used for this analysis.

Charged particles reconstructed using the combined information from the ITS and TPC in $|\eta| < 0.8$ and $0.2 < p_{\text{T}} < 5.0$ GeV/c are selected with full azimuthal coverage. Additional quality cuts are applied to reduce the contamination from secondary charged particles (i.e. particles originating from weak decays, conversions and secondary hadronic interactions in the detector material) and fake tracks (with random associations of space points). Only tracks with at least 70 space points in the TPC (out of a maximum of 159) with an average χ^2 per degree-of-freedom for the track fit lower than 2, a distance of closest approach (DCA) to the reconstructed event vertex smaller than 2.4 cm in the transverse plane (xy) and 3.2 cm in the longitudinal direction (z) are accepted. The charged particle track reconstruction efficiency was estimated from HIJING simulations [43, 44] combined with a GEANT3 [45] detector model, and found to be independent of the collision centrality. The reconstruction efficiency, which may bias the determination of the p_{T} averaged charge-dependent correlations and flow, increases from 70% at $p_{\text{T}} = 0.2$ GeV/c to 85% at $p_{\text{T}} \sim 1.5$ GeV/c where it has a maximum. It then gradually decreases and is flat at 80% for $p_{\text{T}} > 3.0$ GeV/c. The systematic uncertainty of the efficiency is about 5%.

The event shape selection is performed as in [30] based on the magnitude of the second-order reduced flow vector, q_2 [46], defined as

$$q_2 = \frac{|\mathbf{Q}_2|}{\sqrt{M}}, \quad (4)$$

where $|\mathbf{Q}_2| = \sqrt{Q_{2,x}^2 + Q_{2,y}^2}$ is the magnitude of the second order harmonic flow vector and M is the mul-

	Opposite charge	Same charge
$\delta_{\alpha\beta}$	$(3.4 - 25) \times 10^{-5}$	$(3.1 - 10) \times 10^{-5}$
$\gamma_{\alpha\beta}$	$(2.6 - 34) \times 10^{-6}$	$(4.1 - 74) \times 10^{-6}$
v_2	$(1.2 - 4.7) \times 10^{-3}$	

Table 1: Summary of absolute systematic uncertainties. The uncertainties depend on centrality and shape selection, whose minimum and maximum values are listed here.

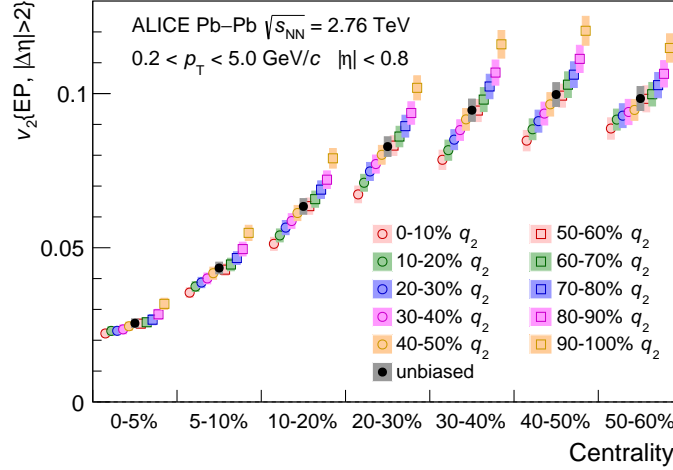


Fig. 1: (Colour online) Unidentified charged particle v_2 for shape selected and unbiased events as a function of collision centrality. The event selection is based on q_2 determined in the V0C with the lowest (highest) value corresponding to 0–10% (90–100%) q_2 . Points are slightly shifted along the horizontal axis for better visibility. Error bars (shaded boxes) represent the statistical (systematic) uncertainties.

tiplicity. The vector \mathbf{Q}_2 is calculated from the azimuthal distribution of the energy deposition measured in the V0C. Its x and y components and the multiplicity are given by

$$Q_{2,x} = \sum_i w_i \cos(2\varphi_i), \quad Q_{2,y} = \sum_i w_i \sin(2\varphi_i), \quad M = \sum_i w_i, \quad (5)$$

where the sum runs over all channels i of the V0C detector ($i = 1 - 32$), φ_i is the azimuthal angle of channel i and w_i is the amplitude measured in channel i . The large gap in pseudorapidity ($|\Delta\eta| > 0.9$) between the charged particles in the TPC used to determine v_2 , $\delta_{\alpha\beta}$ and $\gamma_{\alpha\beta}$ and those in the V0C suppresses non-flow effects. Ten event-shape classes with the lowest (highest) q_2 value corresponding to 0–10% (90–100%) q_2 are investigated for each centrality interval.

The flow coefficient v_2 is measured using the event plane method [16]. The orientation of the event plane $\Psi_{2,EP}$ is estimated from the azimuthal distribution of the energy deposition measured by the V0A detector. The event plane resolution is calculated from correlations between the event planes determined in the TPC and the two V0 detectors separately [16]. The non-flow contributions to the v_2 coefficient and charge-dependent azimuthal correlations are greatly suppressed by the large rapidity separation between the TPC and the V0A ($|\Delta\eta| > 2.0$).

The absolute systematic uncertainties are evaluated from the variation of the results with different selection criteria on the reconstructed collision vertex, different magnetic field polarities, as well as by estimating the centrality from multiplicities measured by the TPC or the SPD rather than the V0 detector. Changes of the results due to variations of the track-selection criteria (e.g. changing the DCA xy and z ranges, number of the TPC space points, using tracks reconstructed by the TPC only) are considered as part of the systematic uncertainties. The effect of reconstruction efficiency on the measurements

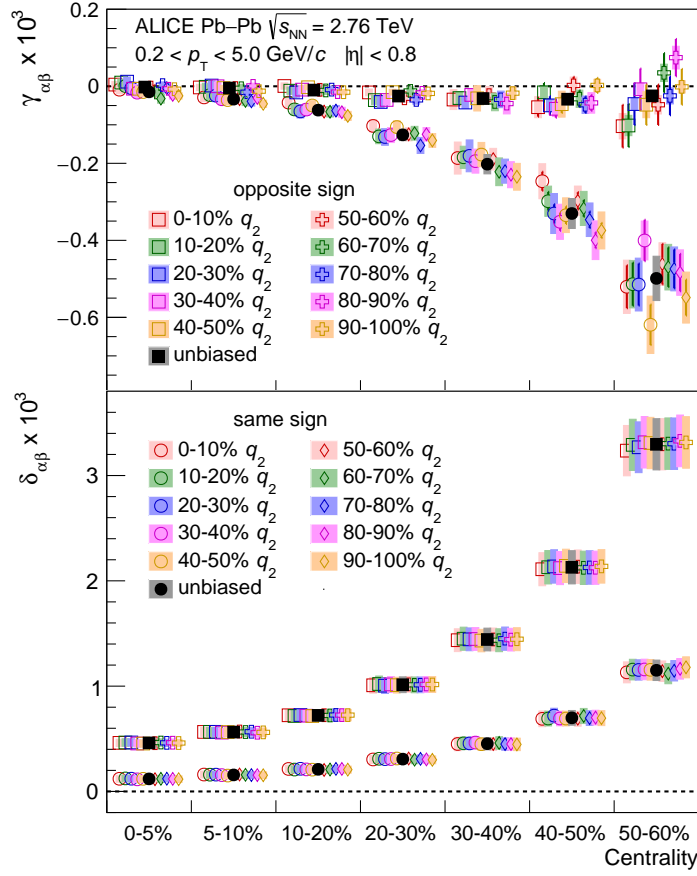


Fig. 2: (Colour online) Top: Centrality dependence of $\gamma_{\alpha\beta}$ for pairs of particles with same and opposite charge for shape selected and unbiased events. Bottom: Centrality dependence of $\delta_{\alpha\beta}$ for pairs of particles with same and opposite charge for shape selected and unbiased events. The event selection is based on q_2 determined in the V0C with the lowest (highest) value corresponding to 0–10% (90–100%) q_2 . Points are slightly shifted along the horizontal axis for better visibility in both panels. Error bars (shaded boxes) represent the statistical (systematic) uncertainties.

is checked by randomly rejecting tracks to ensure a flat acceptance in p_T . The detector response is studied using HIJING and AMPT [47] simulations, where the v_2 coefficients and the charge-dependent azimuthal correlations obtained directly from the models are compared with those from reconstructed tracks. The largest contribution to the systematic uncertainties is given by the detector response. The checks related to the reconstruction efficiency, magnetic field polarity and track-selection criteria also yield significant deviations from the nominal values for v_2 , $\gamma_{\alpha\beta}$ and $\delta_{\alpha\beta}$, respectively. The contributions from all sources are added in quadrature as an estimate of the total systematic uncertainty. The resulting systematic uncertainties are summarized in Table 1.

Figure 1 presents the unidentified charged particle v_2 averaged over $0.2 < p_T < 5.0$ GeV/c for shape selected and unbiased samples as a function of collision centrality. The measured v_2 for the shape selected events differs from the average by up to 25%, which demonstrates that events with the desired initial spatial anisotropy can be experimentally selected. Sensitivity of the event shape selection deteriorates for peripheral collisions due to the low multiplicity and for central collisions due to the reduced magnitude of flow [30].

The centrality dependence of $\gamma_{\alpha\beta}$ for pairs of particles with same and opposite charge for shape selected and unbiased events is shown in the top panel of Fig. 2. The same charge results denote the average

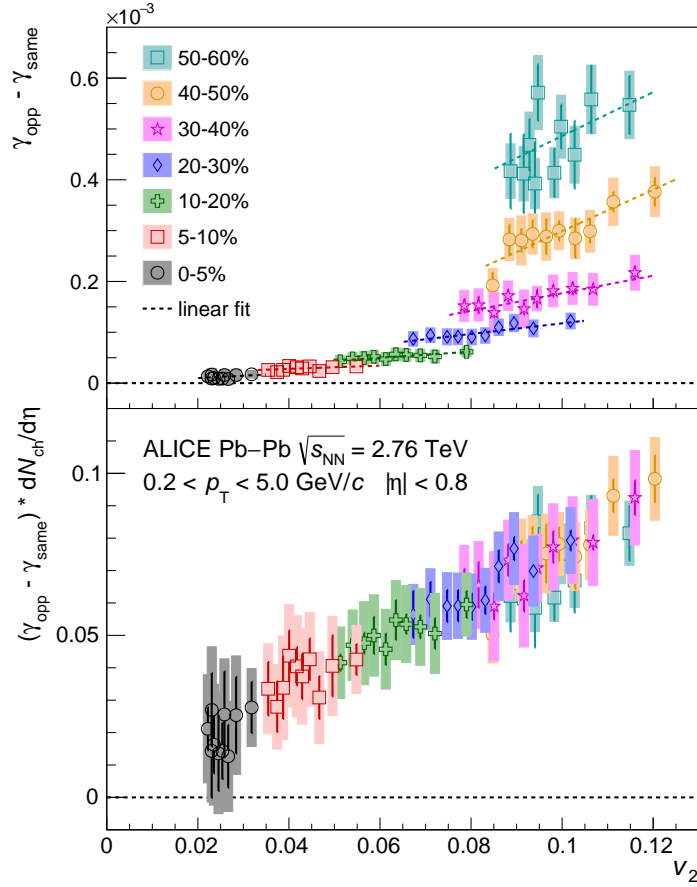


Fig. 3: (Colour online) Top: Difference between opposite and same charge pair correlations for $\gamma_{\alpha\beta}$ as a function of v_2 for shape selected events together with a linear fit (dashed lines) for various centrality classes. Bottom: Difference between opposite and same charge pair correlations for $\gamma_{\alpha\beta}$ multiplied by the charged-particle density [48] as a function of v_2 for shape selected events for various centrality classes. The event selection is based on q_2 determined in the V0C with the lowest (highest) value corresponding to 0–10% (90–100%) q_2 . Error bars (shaded boxes) represent the statistical (systematic) uncertainties.

between pairs of particles with only positive and only negative charges since the two combinations are found to be consistent within statistical uncertainties. The correlation of pairs with the same charge is stronger than the correlation for pairs of opposite charge for both shape selected and unbiased events. The ordering of the correlations of pairs with same and opposite charge indicates a charge separation with respect to the reaction plane. The magnitude of the same and opposite charge pair correlations depends weakly on the event shape selection (q_2 , i.e. v_2) in a given centrality bin.

The bottom panel of Fig. 2 shows the centrality dependence of $\delta_{\alpha\beta}$ for pairs of particles with same and opposite charge for shape selected and unbiased samples. As reported in [27], the magnitude of the correlation for the same charge pairs is smaller than for the opposite charge combinations. This is in contrast to the CME expectation, indicating that background dominates the correlations. The same and opposite charge pair correlations are insensitive to the event-shape selection in a given centrality bin.

The difference between opposite and same charge pair correlations for $\gamma_{\alpha\beta}$ can be used to study the charge separation effect. This difference is presented as a function of v_2 for various centrality classes in the top panel of Fig. 3. The difference is positive for all centralities and its magnitude decreases for more central collisions and with decreasing v_2 (in a given centrality bin). At least two effects could be

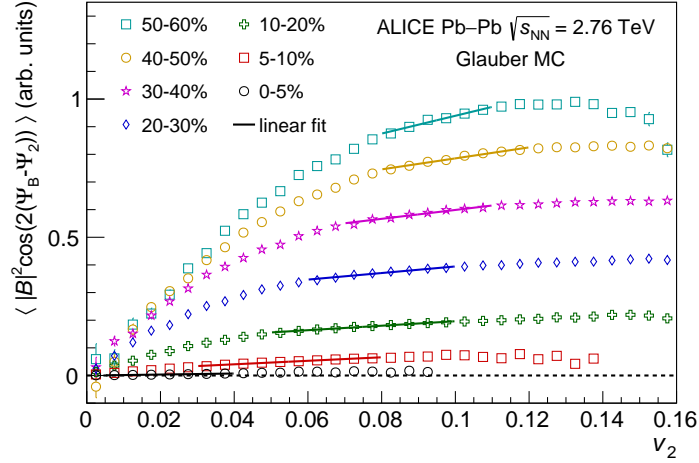


Fig. 4: (Colour online) The expected dependence of the CME signal on v_2 for various centrality classes from a MC-Glauber simulation [50] (see text for details). No event shape selection is performed in the model, and therefore a large range in v_2 is covered. The solid lines depict linear fits based on the v_2 variation observed within each centrality interval.

responsible for the centrality dependence: the reduction of the magnetic field with decreasing centrality and the dilution of the correlation due to the increase in the number of particles [24] in more central collisions. The difference between opposite and same charge pair correlations multiplied by the charged-particle density in a given centrality bin, $dN_{ch}/d\eta$ (taken from [48]), to compensate for the dilution effect, is presented as a function of v_2 in the bottom panel of Fig. 3. All the data points fall approximately onto the same line. This is qualitatively consistent with expectations from LCC where an increase in v_2 , which modulates the correlation between balancing charges with respect to the reaction plane [49], results in a strong effect. Therefore, the observed dependence on v_2 points to a large background contribution to $\gamma_{\alpha\beta}$.

The expected dependence of the CME signal on v_2 was evaluated with the help of a Monte Carlo Glauber [50] calculation including a magnetic field. In this simulation, the centrality classes are determined from the multiplicity of charged particles in the acceptance of the V0 detector following the method presented in [42]. The multiplicity is generated according to a negative binomial distribution with parameters taken from [42] based on the number of participant nucleons and binary collisions. The elliptic flow is assumed to be proportional to the eccentricity of the participant nucleons and approximately reproduces the measured p_T -integrated v_2 values [51]. The magnetic field is evaluated at the geometrical center of the overlap region from the number of spectator nucleons following Eq. (A.6) from [11] with the proper time $\tau = 0.1$ fm/c. The magnetic field is calculated in 1% centrality classes and averaged into the centrality intervals used for data analysis. It is assumed that the CME signal is proportional to $\langle |B|^2 \cos(2(\Psi_B - \Psi_2)) \rangle$, where $|B|$ and Ψ_B are the magnitude and direction of the magnetic field, respectively. Figure 4 presents the expected dependence of the CME signal on v_2 for various centrality classes. Similar results are found using MC-KLN CGC [52, 53] and EKRT [54] initial conditions. The MC-KLN CGC simulation was performed using version 32 of the Monte Carlo k_T -factorization code (*mckt*) available at [55], while the TRENTO model [56] was employed for EKRT initial conditions.

To disentangle the potential CME signal from background, the dependence on v_2 of the difference between opposite and same charge pair correlations for $\gamma_{\alpha\beta}$ and the CME signal expectations are fitted with a linear function (see lines in Figs. 3 (top panel) and 4, respectively):

$$F_1(v_2) = p_0(1 + p_1(v_2 - \langle v_2 \rangle) / \langle v_2 \rangle), \quad (6)$$

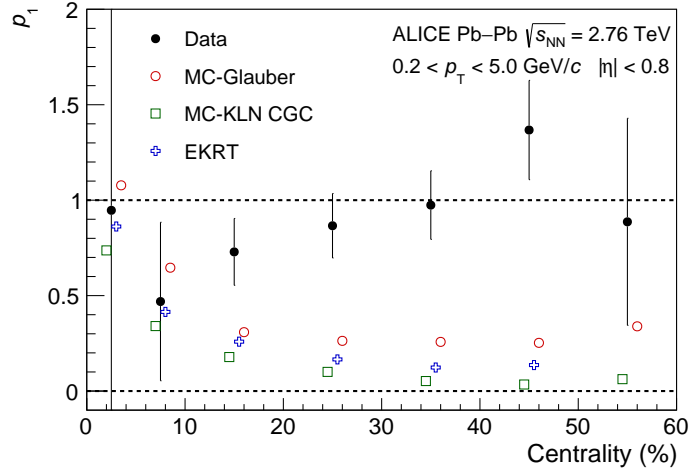


Fig. 5: (Colour online) Centrality dependence of the p_1 parameter from a linear fit to the difference between opposite and same charge pair correlations for $\gamma_{\alpha\beta}$ and from linear fits to the CME signal expectations from MC-Glauber [50], MC-KLN CGC [52, 53] and EKRT [54] models (see text for details). Points from MC simulations are slightly shifted along the horizontal axis for better visibility. Only statistical uncertainties are shown.

where p_0 accounts for the overall scale, which cannot be fixed in the MC calculations, and p_1 reflects the slope in the signal normalised to unity at $v_2 = \langle v_2 \rangle$. In a pure background scenario, the correlator is directly proportional to v_2 and the p_1 parameter is equal to unity. The presence of a significant CME contribution, on the other hand, would result in non-zero intercepts at $v_2 = 0$ of the linear functions shown in Fig. 3. The ranges used in these fits are based on the v_2 variation observed within each centrality interval. The centrality dependence of p_1 from fits to data and to the signal expectations based on MC-Glauber, MC-KLN CGC and EKRT models is reported in Fig. 5. In this case, p_1 from data and MC models can be related according to

$$f_{\text{CME}} \times p_{1,\text{MC}} + (1 - f_{\text{CME}}) \times 1 = p_{1,\text{data}}, \quad (7)$$

where f_{CME} denotes the CME fraction to the charge dependence of $\gamma_{\alpha\beta}$ and is given by

$$f_{\text{CME}} = \frac{(\gamma_{\text{opp}} - \gamma_{\text{same}})^{\text{CME}}}{(\gamma_{\text{opp}} - \gamma_{\text{same}})^{\text{CME}} + (\gamma_{\text{opp}} - \gamma_{\text{same}})^{\text{Bkg}}}. \quad (8)$$

Figure 6 presents f_{CME} for the three models used in this study. The CME fraction cannot be extracted for central (0–10%) and peripheral (50–60%) collisions due to the large statistical uncertainties on p_1 extracted from data. The negative values for the CME fraction obtained for the 40–50% centrality range (deviating from zero by one σ), if confirmed, would indicate that our expectations for the background contribution to be linearly proportional to v_2 are not accurate. Combining the points from 10–50% neglecting a possible centrality dependence gives $f_{\text{CME}} = 0.10 \pm 0.13$, $f_{\text{CME}} = 0.08 \pm 0.10$ and $f_{\text{CME}} = 0.08 \pm 0.11$ for the MC-Glauber, MC-KLN CGC and EKRT models, respectively. These results are consistent with zero CME fraction and correspond to upper limits on f_{CME} of 33%, 26% and 29%, respectively, at 95% confidence level for the 10–50% centrality interval. The CME fraction agrees with the observations in [36] where the centrality intervals overlap.

In summary, the Event Shape Engineering technique has been applied to measure the dependence on v_2 of the charge-dependent two- and three-particle correlators $\delta_{\alpha\beta}$ and $\gamma_{\alpha\beta}$ in Pb–Pb collisions at $\sqrt{s_{\text{NN}}} = 2.76$ TeV. While for $\delta_{\alpha\beta}$ we observe no significant v_2 dependence in a given centrality bin, $\gamma_{\alpha\beta}$ is found to be almost linearly dependent on v_2 . When multiplied by the corresponding charged-particle density,

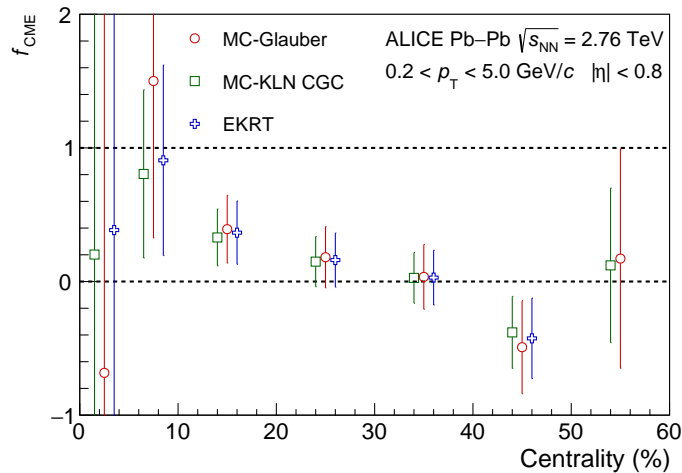


Fig. 6: (Colour online) Centrality dependence of the CME fraction extracted from the slope parameter of fits to data and MC-Glauber [50], MC-KLN CGC [52, 53] and EKRT [54] models, respectively (see text for details). The dashed lines indicate the physical parameter space of the CME fraction. Points are slightly shifted along the horizontal axis for better visibility. Only statistical uncertainties are shown.

to compensate for the dilution effect, a linear dependence is observed consistently across all centrality classes. Using a Monte Carlo simulation with different initial-state models, we have found that the CME signal is expected to exhibit a weak dependence on v_2 . These observations imply that the dominant contribution to $\gamma_{\alpha\beta}$ is due to non-CME effects. In order to get a quantitative estimate of the signal and background contributions to the measurements, we fit both $\gamma_{\alpha\beta}$ and the expected signal dependence on v_2 with a first order polynomial. This allows the resulting fraction of the CME signal to be estimated in the centrality range 10–50%, but not for the most central (0–10%) and peripheral (50–60%) collisions due to large statistical uncertainties. Averaging over the centrality range 10–50% gives an upper limit of 26% to 33% (depending on the initial-state model) at 95% confidence level for the CME contribution to the difference between opposite and same charge pair correlations for $\gamma_{\alpha\beta}$.

Acknowledgements

The ALICE Collaboration would like to thank all its engineers and technicians for their invaluable contributions to the construction of the experiment and the CERN accelerator teams for the outstanding performance of the LHC complex. The ALICE Collaboration gratefully acknowledges the resources and support provided by all Grid centres and the Worldwide LHC Computing Grid (WLCG) collaboration. The ALICE Collaboration acknowledges the following funding agencies for their support in building and running the ALICE detector: A. I. Alikhanyan National Science Laboratory (Yerevan Physics Institute) Foundation (ANSL), State Committee of Science and World Federation of Scientists (WFS), Armenia; Austrian Academy of Sciences and Nationalstiftung für Forschung, Technologie und Entwicklung, Austria; Ministry of Communications and High Technologies, National Nuclear Research Center, Azerbaijan; Conselho Nacional de Desenvolvimento Científico e Tecnológico (CNPq), Universidade Federal do Rio Grande do Sul (UFRGS), Financiadora de Estudos e Projetos (Finep) and Fundação de Amparo à Pesquisa do Estado de São Paulo (FAPESP), Brazil; Ministry of Science & Technology of China (MSTC), National Natural Science Foundation of China (NSFC) and Ministry of Education of China (MOEC), China; Ministry of Science, Education and Sport and Croatian Science Foundation, Croatia; Ministry of Education, Youth and Sports of the Czech Republic, Czech Republic; The Danish Council for Independent Research — Natural Sciences, the Carlsberg Foundation and Danish National Research Foundation (DNRF), Denmark; Helsinki Institute of Physics (HIP), Finland; Commissariat à l’Energie

Atomique (CEA) and Institut National de Physique Nucléaire et de Physique des Particules (IN2P3) and Centre National de la Recherche Scientifique (CNRS), France; Bundesministerium für Bildung, Wissenschaft, Forschung und Technologie (BMBF) and GSI Helmholtzzentrum für Schwerionenforschung GmbH, Germany; General Secretariat for Research and Technology, Ministry of Education, Research and Religions, Greece; National Research, Development and Innovation Office, Hungary; Department of Atomic Energy Government of India (DAE) and Council of Scientific and Industrial Research (CSIR), New Delhi, India; Indonesian Institute of Science, Indonesia; Centro Fermi - Museo Storico della Fisica e Centro Studi e Ricerche Enrico Fermi and Istituto Nazionale di Fisica Nucleare (INFN), Italy; Institute for Innovative Science and Technology, Nagasaki Institute of Applied Science (IIST), Japan Society for the Promotion of Science (JSPS) KAKENHI and Japanese Ministry of Education, Culture, Sports, Science and Technology (MEXT), Japan; Consejo Nacional de Ciencia (CONACYT) y Tecnología, through Fondo de Cooperación Internacional en Ciencia y Tecnología (FONCICYT) and Dirección General de Asuntos del Personal Académico (DGAPA), Mexico; Nederlandse Organisatie voor Wetenschappelijk Onderzoek (NWO), Netherlands; The Research Council of Norway, Norway; Commission on Science and Technology for Sustainable Development in the South (COMSATS), Pakistan; Pontificia Universidad Católica del Perú, Peru; Ministry of Science and Higher Education and National Science Centre, Poland; Korea Institute of Science and Technology Information and National Research Foundation of Korea (NRF), Republic of Korea; Ministry of Education and Scientific Research, Institute of Atomic Physics and Romanian National Agency for Science, Technology and Innovation, Romania; Joint Institute for Nuclear Research (JINR), Ministry of Education and Science of the Russian Federation and National Research Centre Kurchatov Institute, Russia; Ministry of Education, Science, Research and Sport of the Slovak Republic, Slovakia; National Research Foundation of South Africa, South Africa; Centro de Aplicaciones Tecnológicas y Desarrollo Nuclear (CEADEN), Cubaenergía, Cuba, Ministerio de Ciencia e Innovación and Centro de Investigaciones Energéticas, Medioambientales y Tecnológicas (CIEMAT), Spain; Swedish Research Council (VR) and Knut & Alice Wallenberg Foundation (KAW), Sweden; European Organization for Nuclear Research, Switzerland; National Science and Technology Development Agency (NSDTA), Suranaree University of Technology (SUT) and Office of the Higher Education Commission under NRU project of Thailand, Thailand; Turkish Atomic Energy Agency (TAEK), Turkey; National Academy of Sciences of Ukraine, Ukraine; Science and Technology Facilities Council (STFC), United Kingdom; National Science Foundation of the United States of America (NSF) and United States Department of Energy, Office of Nuclear Physics (DOE NP), United States of America.

References

- [1] T. D. Lee, “A Theory of Spontaneous T Violation,” *Phys. Rev.* **D8** (1973) 1226–1239.
- [2] T. D. Lee and G. C. Wick, “Vacuum Stability and Vacuum Excitation in a Spin 0 Field Theory,” *Phys. Rev.* **D9** (1974) 2291–2316.
- [3] P. D. Morley and I. A. Schmidt, “Strong P, CP, T Violations in Heavy Ion Collisions,” *Z. Phys.* **C26** (1985) 627.
- [4] D. Kharzeev, R. D. Pisarski, and M. H. G. Tytgat, “Possibility of spontaneous parity violation in hot QCD,” *Phys. Rev. Lett.* **81** (1998) 512–515, arXiv:hep-ph/9804221 [hep-ph].
- [5] S.-S. Chern and J. Simons, “Characteristic forms and geometric invariants,” *Annals Math.* **99** (1974) 48–69.
- [6] A. Bzdak and V. Skokov, “Event-by-event fluctuations of magnetic and electric fields in heavy ion collisions,” *Phys. Lett.* **B710** (2012) 171–174, arXiv:1111.1949 [hep-ph].
- [7] W.-T. Deng and X.-G. Huang, “Event-by-event generation of electromagnetic fields in heavy-ion collisions,” *Phys. Rev.* **C85** (2012) 044907, arXiv:1201.5108 [nucl-th].

- [8] U. Gursoy, D. Kharzeev, and K. Rajagopal, “Magnetohydrodynamics, charged currents and directed flow in heavy ion collisions,” *Phys. Rev.* **C89** no. 5, (2014) 054905, arXiv:1401.3805 [hep-ph].
- [9] D. Kharzeev, “Parity violation in hot QCD: Why it can happen, and how to look for it,” *Phys. Lett.* **B633** (2006) 260–264, arXiv:hep-ph/0406125 [hep-ph].
- [10] D. Kharzeev and A. Zhitnitsky, “Charge separation induced by P-odd bubbles in QCD matter,” *Nucl. Phys.* **A797** (2007) 67–79, arXiv:0706.1026 [hep-ph].
- [11] D. E. Kharzeev, L. D. McLerran, and H. J. Warringa, “The Effects of topological charge change in heavy ion collisions: ‘Event by event P and CP violation’,” *Nucl. Phys.* **A803** (2008) 227–253, arXiv:0711.0950 [hep-ph].
- [12] K. Fukushima, D. E. Kharzeev, and H. J. Warringa, “The Chiral Magnetic Effect,” *Phys. Rev.* **D78** (2008) 074033, arXiv:0808.3382 [hep-ph].
- [13] S. A. Voloshin, A. M. Poskanzer, and R. Snellings, “Collective phenomena in non-central nuclear collisions,” arXiv:0809.2949 [nucl-ex].
- [14] U. Heinz and R. Snellings, “Collective flow and viscosity in relativistic heavy-ion collisions,” *Ann. Rev. Nucl. Part. Sci.* **63** (2013) 123–151, arXiv:1301.2826 [nucl-th].
- [15] S. Voloshin and Y. Zhang, “Flow study in relativistic nuclear collisions by Fourier expansion of Azimuthal particle distributions,” *Z. Phys.* **C70** (1996) 665–672, arXiv:hep-ph/9407282 [hep-ph].
- [16] A. M. Poskanzer and S. A. Voloshin, “Methods for analyzing anisotropic flow in relativistic nuclear collisions,” *Phys. Rev.* **C58** (1998) 1671–1678, arXiv:nucl-ex/9805001 [nucl-ex].
- [17] S. A. Voloshin, “Parity violation in hot QCD: How to detect it,” *Phys. Rev.* **C70** (2004) 057901, arXiv:hep-ph/0406311 [hep-ph].
- [18] S. Schlichting and S. Pratt, “Charge conservation at energies available at the BNL Relativistic Heavy Ion Collider and contributions to local parity violation observables,” *Phys. Rev.* **C83** (2011) 014913, arXiv:1009.4283 [nucl-th].
- [19] S. Pratt, S. Schlichting, and S. Gavin, “Effects of Momentum Conservation and Flow on Angular Correlations at RHIC,” *Phys. Rev.* **C84** (2011) 024909, arXiv:1011.6053 [nucl-th].
- [20] J. Liao, V. Koch, and A. Bzdak, “On the Charge Separation Effect in Relativistic Heavy Ion Collisions,” *Phys. Rev.* **C82** (2010) 054902, arXiv:1005.5380 [nucl-th].
- [21] A. Bzdak, V. Koch, and J. Liao, “Azimuthal correlations from transverse momentum conservation and possible local parity violation,” *Phys. Rev.* **C83** (2011) 014905, arXiv:1008.4919 [nucl-th].
- [22] D. Teaney and L. Yan, “Triangularity and Dipole Asymmetry in Heavy Ion Collisions,” *Phys. Rev.* **C83** (2011) 064904, arXiv:1010.1876 [nucl-th].
- [23] **STAR** Collaboration, B. I. Abelev *et al.*, “Azimuthal Charged-Particle Correlations and Possible Local Strong Parity Violation,” *Phys. Rev. Lett.* **103** (2009) 251601, arXiv:0909.1739 [nucl-ex].
- [24] **STAR** Collaboration, B. I. Abelev *et al.*, “Observation of charge-dependent azimuthal correlations and possible local strong parity violation in heavy ion collisions,” *Phys. Rev.* **C81** (2010) 054908, arXiv:0909.1717 [nucl-ex].

- [25] **STAR** Collaboration, L. Adamczyk *et al.*, “Fluctuations of charge separation perpendicular to the event plane and local parity violation in $\sqrt{s_{NN}} = 200$ GeV Au+Au collisions at the BNL Relativistic Heavy Ion Collider,” *Phys. Rev.* **C88** no. 6, (2013) 064911, arXiv:1302.3802 [nucl-ex].
- [26] **STAR** Collaboration, L. Adamczyk *et al.*, “Beam-energy dependence of charge separation along the magnetic field in Au+Au collisions at RHIC,” *Phys. Rev. Lett.* **113** (2014) 052302, arXiv:1404.1433 [nucl-ex].
- [27] **ALICE** Collaboration, B. Abelev *et al.*, “Charge separation relative to the reaction plane in Pb-Pb collisions at $\sqrt{s_{NN}} = 2.76$ TeV,” *Phys. Rev. Lett.* **110** no. 1, (2013) 012301, arXiv:1207.0900 [nucl-ex].
- [28] **ALICE** Collaboration, J. Adam *et al.*, “Charge-dependent flow and the search for the chiral magnetic wave in Pb-Pb collisions at $\sqrt{s_{NN}} = 2.76$ TeV,” *Phys. Rev.* **C93** no. 4, (2016) 044903, arXiv:1512.05739 [nucl-ex].
- [29] J. Schukraft, A. Timmins, and S. A. Voloshin, “Ultra-relativistic nuclear collisions: event shape engineering,” *Phys. Lett.* **B719** (2013) 394–398, arXiv:1208.4563 [nucl-ex].
- [30] **ALICE** Collaboration, J. Adam *et al.*, “Event shape engineering for inclusive spectra and elliptic flow in Pb-Pb collisions at $\sqrt{s_{NN}}=2.76$ TeV,” *Phys. Rev.* **C93** no. 3, (2016) 034916, arXiv:1507.06194 [nucl-ex].
- [31] **ATLAS** Collaboration, G. Aad *et al.*, “Measurement of the correlation between flow harmonics of different order in lead-lead collisions at $\sqrt{s_{NN}}=2.76$ TeV with the ATLAS detector,” *Phys. Rev.* **C92** no. 3, (2015) 034903, arXiv:1504.01289 [hep-ex].
- [32] F. G. Gardim, F. Grassi, M. Luzum, and J.-Y. Ollitrault, “Mapping the hydrodynamic response to the initial geometry in heavy-ion collisions,” *Phys. Rev.* **C85** (2012) 024908, arXiv:1111.6538 [nucl-th].
- [33] A. Bzdak, “Suppression of elliptic flow induced correlations in an observable of possible local parity violation,” *Phys. Rev.* **C85** (2012) 044919, arXiv:1112.4066 [nucl-th].
- [34] **CMS** Collaboration, V. Khachatryan *et al.*, “Observation of charge-dependent azimuthal correlations in p -Pb collisions and its implication for the search for the chiral magnetic effect,” *Phys. Rev. Lett.* **118** no. 12, (2017) 122301, arXiv:1610.00263 [nucl-ex].
- [35] R. Belmont and J. L. Nagle, “To CME or not to CME? Implications of p +Pb measurements of the chiral magnetic effect in heavy ion collisions,” *Phys. Rev.* **C96** no. 2, (2017) 024901, arXiv:1610.07964 [nucl-th].
- [36] **CMS** Collaboration, A. M. Sirunyan *et al.*, “Constraints on the chiral magnetic effect using charge-dependent azimuthal correlations in p Pb and PbPb collisions at the LHC,” arXiv:1708.01602 [nucl-ex].
- [37] **ALICE** Collaboration, K. Aamodt *et al.*, “The ALICE experiment at the CERN LHC,” *JINST* **3** (2008) S08002.
- [38] **ALICE** Collaboration, B. B. Abelev *et al.*, “Performance of the ALICE Experiment at the CERN LHC,” *Int. J. Mod. Phys.* **A29** (2014) 1430044, arXiv:1402.4476 [nucl-ex].
- [39] J. Alme *et al.*, “The ALICE TPC, a large 3-dimensional tracking device with fast readout for ultra-high multiplicity events,” *Nucl. Instrum. Meth.* **A622** (2010) 316–367, arXiv:1001.1950 [physics.ins-det].

- [40] **ALICE** Collaboration, K. Aamodt *et al.*, “Alignment of the ALICE Inner Tracking System with cosmic-ray tracks,” *JINST* **5** (2010) P03003, arXiv:1001.0502 [physics.ins-det].
- [41] **ALICE** Collaboration, E. Abbas *et al.*, “Performance of the ALICE VZERO system,” *JINST* **8** (2013) P10016, arXiv:1306.3130 [nucl-ex].
- [42] **ALICE** Collaboration, B. Abelev *et al.*, “Centrality determination of Pb-Pb collisions at $\sqrt{s_{NN}} = 2.76$ TeV with ALICE,” *Phys. Rev.* **C88** no. 4, (2013) 044909, arXiv:1301.4361 [nucl-ex].
- [43] X.-N. Wang and M. Gyulassy, “HIJING: A Monte Carlo model for multiple jet production in p p, p A and A A collisions,” *Phys. Rev.* **D44** (1991) 3501–3516.
- [44] M. Gyulassy and X.-N. Wang, “HIJING 1.0: A Monte Carlo program for parton and particle production in high-energy hadronic and nuclear collisions,” *Comput. Phys. Commun.* **83** (1994) 307, arXiv:nucl-th/9502021 [nucl-th].
- [45] R. Brun, F. Bruyant, F. Carminati, S. Giani, M. Maire, A. McPherson, G. Patrick, and L. Urban, “GEANT Detector Description and Simulation Tool,” *CERN-W5013* **1** (1994) 1.
- [46] **STAR** Collaboration, C. Adler *et al.*, “Elliptic flow from two and four particle correlations in Au+Au collisions at $\sqrt{s_{NN}} = 130$ GeV,” *Phys. Rev.* **C66** (2002) 034904, arXiv:nucl-ex/0206001 [nucl-ex].
- [47] Z.-W. Lin, C. M. Ko, B.-A. Li, B. Zhang, and S. Pal, “A Multi-phase transport model for relativistic heavy ion collisions,” *Phys. Rev.* **C72** (2005) 064901, arXiv:nucl-th/0411110 [nucl-th].
- [48] **ALICE** Collaboration, K. Aamodt *et al.*, “Centrality dependence of the charged-particle multiplicity density at mid-rapidity in Pb-Pb collisions at $\sqrt{s_{NN}} = 2.76$ TeV,” *Phys. Rev. Lett.* **106** (2011) 032301, arXiv:1012.1657 [nucl-ex].
- [49] Y. Hori, T. Gunji, H. Hamagaki, and S. Schlichting, “Collective flow effects on charge balance correlations and local parity-violation observables in $\sqrt{s_{NN}} = 2.76$ TeV Pb+Pb collisions at the LHC,” arXiv:1208.0603 [nucl-th].
- [50] M. L. Miller, K. Reygers, S. J. Sanders, and P. Steinberg, “Glauber modeling in high energy nuclear collisions,” *Ann. Rev. Nucl. Part. Sci.* **57** (2007) 205–243, arXiv:nucl-ex/0701025 [nucl-ex].
- [51] **ALICE** Collaboration, K. Aamodt *et al.*, “Elliptic flow of charged particles in Pb-Pb collisions at 2.76 TeV,” *Phys. Rev. Lett.* **105** (2010) 252302, arXiv:1011.3914 [nucl-ex].
- [52] H.-J. Drescher and Y. Nara, “Eccentricity fluctuations from the color glass condensate at RHIC and LHC,” *Phys. Rev.* **C76** (2007) 041903, arXiv:0707.0249 [nucl-th].
- [53] J. L. Albacete and A. Dumitru, “A model for gluon production in heavy-ion collisions at the LHC with rcBK unintegrated gluon densities,” arXiv:1011.5161 [hep-ph].
- [54] H. Niemi, K. J. Eskola, and R. Paatelainen, “Event-by-event fluctuations in a perturbative QCD + saturation + hydrodynamics model: Determining QCD matter shear viscosity in ultrarelativistic heavy-ion collisions,” *Phys. Rev.* **C93** no. 2, (2016) 024907, arXiv:1505.02677 [hep-ph].
- [55] http://faculty.baruch.cuny.edu/naturalscience/physics/dumitru/CGC_IC.html.
- [56] J. S. Moreland, J. E. Bernhard, and S. A. Bass, “Alternative ansatz to wounded nucleon and binary collision scaling in high-energy nuclear collisions,” *Phys. Rev.* **C92** no. 1, (2015) 011901, arXiv:1412.4708 [nucl-th].

A The ALICE Collaboration

S. Acharya¹³⁹, J. Adam⁹⁸, D. Adamová⁹⁵, J. Adolfsson³⁴, M.M. Aggarwal¹⁰⁰, G. Aglieri Rinella³⁵, M. Agnello³¹, N. Agrawal⁴⁸, Z. Ahammed¹³⁹, N. Ahmad¹⁷, S.U. Ahn⁸⁰, S. Aiola¹⁴³, A. Akindinov⁶⁵, M. Al-Turany¹⁰⁸, S.N. Alam¹³⁹, D.S.D. Albuquerque¹²⁴, D. Aleksandrov⁹¹, B. Alessandro⁵⁹, R. Alfaro Molina⁷⁵, A. Alici^{27,54,12}, A. Alkin³, J. Alme²², T. Alt⁷¹, L. Altenkamper²², I. Altsybeev¹³⁸, C. Alves Garcia Prado¹²³, C. Andrei⁸⁸, D. Andreou³⁵, H.A. Andrews¹¹², A. Andronic¹⁰⁸, V. Anguelov¹⁰⁵, C. Anson⁹⁸, T. Antičić¹⁰⁹, F. Antinori⁵⁷, P. Antonioli⁵⁴, R. Anwar¹²⁶, L. Aphecetche¹¹⁶, H. Appelshäuser⁷¹, S. Arcelli²⁷, R. Arnaldi⁵⁹, O.W. Arnold^{106,36}, I.C. Arsene²¹, M. Arslanok¹⁰⁵, B. Audurier¹¹⁶, A. Augustinus³⁵, R. Averbeck¹⁰⁸, M.D. Azmi¹⁷, A. Badalà⁵⁶, Y.W. Baek^{61,79}, S. Bagnasco⁵⁹, R. Bailhache⁷¹, R. Bala¹⁰², A. Baldisseri⁷⁶, M. Ball⁴⁵, R.C. Baral^{68,89}, A.M. Barbano²⁶, R. Barbera²⁸, F. Barile^{53,33}, L. Barioglio²⁶, G.G. Barnaföldi¹⁴², L.S. Barnby⁹⁴, V. Barret¹³³, P. Bartalini⁷, K. Barth³⁵, E. Bartsch⁷¹, M. Basile²⁷, N. Bastid¹³³, S. Basu¹⁴¹, G. Batigne¹¹⁶, B. Batyunya⁷⁸, P.C. Batzing²¹, J.L. Bazo Alba¹¹³, I.G. Bearden⁹², H. Beck¹⁰⁵, C. Bedda⁶⁴, N.K. Behera⁶¹, I. Belikov¹³⁵, F. Bellini^{27,35}, H. Bello Martinez², R. Bellwied¹²⁶, L.G.E. Beltran¹²², V. Belyaev⁸⁴, G. Bencedi¹⁴², S. Beole²⁶, A. Bercuci⁸⁸, Y. Berdnikov⁹⁷, D. Berenyi¹⁴², R.A. Bertens¹²⁹, D. Berzano³⁵, L. Betev³⁵, A. Bhasin¹⁰², I.R. Bhat¹⁰², A.K. Bhati¹⁰⁰, B. Bhattacharjee⁴⁴, J. Bhom¹²⁰, A. Bianchi²⁶, L. Bianchi¹²⁶, N. Bianchi⁵¹, C. Bianchin¹⁴¹, J. Bielčík³⁹, J. Bielčíková⁹⁵, A. Bilandzic^{36,106}, G. Biro¹⁴², R. Biswas⁴, S. Biswas⁴, J.T. Blair¹²¹, D. Blau⁹¹, C. Blume⁷¹, G. Boca¹³⁶, F. Bock^{83,35,105}, A. Bogdanov⁸⁴, L. Boldizsár¹⁴², M. Bombara⁴⁰, G. Bonomi¹³⁷, M. Bonora³⁵, J. Book⁷¹, H. Borel⁷⁶, A. Borissov^{105,19}, M. Borri¹²⁸, E. Botta²⁶, C. Bourjau⁹², L. Bratrud⁷¹, P. Braun-Munzinger¹⁰⁸, M. Bregant¹²³, T.A. Broker⁷¹, M. Broz³⁹, E.J. Brucken⁴⁶, E. Bruna⁵⁹, G.E. Bruno^{35,33}, D. Budnikov¹¹⁰, H. Buesching⁷¹, S. Bufalino³¹, P. Buhler¹¹⁵, P. Buncic³⁵, O. Busch¹³², Z. Buthelezi⁷⁷, J.B. Butt¹⁵, J.T. Buxton¹⁸, J. Cabala¹¹⁸, D. Caffarri^{35,93}, H. Caines¹⁴³, A. Caliva^{64,108}, E. Calvo Villar¹¹³, P. Camerini²⁵, A.A. Capon¹¹⁵, F. Carena³⁵, W. Carena³⁵, F. Carnesecchi^{27,12}, J. Castillo Castellanos⁷⁶, A.J. Castro¹²⁹, E.A.R. Casula⁵⁵, C. Ceballos Sanchez⁹, P. Cerello⁵⁹, S. Chandra¹³⁹, B. Chang¹²⁷, S. Chapeland³⁵, M. Chartier¹²⁸, S. Chattopadhyay¹³⁹, S. Chattopadhyay¹¹¹, A. Chauvin^{36,106}, C. Cheshkov¹³⁴, B. Cheynis¹³⁴, V. Chibante Barroso³⁵, D.D. Chinellato¹²⁴, S. Cho⁶¹, P. Chochula³⁵, M. Chojnacki⁹², S. Choudhury¹³⁹, T. Chowdhury¹³³, P. Christakoglou⁹³, C.H. Christensen⁹², P. Christiansen³⁴, T. Chujo¹³², S.U. Chung¹⁹, C. Cicalo⁵⁵, L. Cifarelli^{12,27}, F. Cindolo⁵⁴, J. Cleymans¹⁰¹, F. Colamaria³³, D. Colella^{35,66,53}, A. Collu⁸³, M. Colocci²⁷, M. Concas^{59,ii}, G. Conesa Balbastre⁸², Z. Conesa del Valle⁶², M.E. Connors^{143,iii}, J.G. Contreras³⁹, T.M. Cormier⁹⁶, Y. Corrales Morales⁵⁹, I. Cortés Maldonado², P. Cortese³², M.R. Cosentino¹²⁵, F. Costa³⁵, S. Costanza¹³⁶, J. Crkovič⁶², P. Crochet¹³³, E. Cuautle⁷³, L. Cunqueiro⁷², T. Dahms^{36,106}, A. Dainese⁵⁷, M.C. Danisch¹⁰⁵, A. Danu⁶⁹, D. Das¹¹¹, I. Das¹¹¹, S. Das⁴, A. Dash⁸⁹, S. Dash⁴⁸, S. De^{49,123}, A. De Caro³⁰, G. de Cataldo⁵³, C. de Conti¹²³, J. de Cuveland⁴², A. De Falco²⁴, D. De Gruttola^{30,12}, N. De Marco⁵⁹, S. De Pasquale³⁰, R.D. De Souza¹²⁴, H.F. Degenhardt¹²³, A. Deisting^{108,105}, A. Deloff⁸⁷, C. Deplano⁹³, P. Dhankher⁴⁸, D. Di Bari³³, A. Di Mauro³⁵, P. Di Nezza⁵¹, B. Di Ruzza⁵⁷, M.A. Diaz Corchero¹⁰, T. Dietel¹⁰¹, P. Dillenseger⁷¹, R. Diviá³⁵, Ø. Djuvsland²², A. Dobrin³⁵, D. Domenicis Gimenez¹²³, B. Dönigus⁷¹, O. Dordic²¹, L.V.R. Doremalen⁶⁴, A.K. Dubey¹³⁹, A. Dubla¹⁰⁸, L. Ducroux¹³⁴, A.K. Duggal¹⁰⁰, M. Dukhishyam⁸⁹, P. Dupieux¹³³, R.J. Ehlers¹⁴³, D. Elia⁵³, E. Endress¹¹³, H. Engel⁷⁰, E. Epple¹⁴³, B. Erazmus¹¹⁶, F. Erhardt⁹⁹, B. Espagnon⁶², S. Esumi¹³², G. Eulisse³⁵, J. Eum¹⁹, D. Evans¹¹², S. Evdokimov¹¹⁴, L. Fabbietti^{106,36}, J. Faivre⁸², A. Fantoni⁵¹, M. Fasel^{96,83}, L. Feldkamp⁷², A. Feliciello⁵⁹, G. Feofilov¹³⁸, A. Fernández Téllez², E.G. Ferreira¹⁶, A. Ferretti²⁶, A. Festanti^{29,35}, V.J.G. Feuillard^{76,133}, J. Figiel¹²⁰, M.A.S. Figueredo¹²³, S. Filchagin¹¹⁰, D. Finogeev⁶³, F.M. Fionda^{22,24}, M. Floris³⁵, S. Foertsch⁷⁷, P. Foka¹⁰⁸, S. Fokin⁹¹, E. Fragiaco⁶⁰, A. Francescon³⁵, A. Francisco¹¹⁶, U. Frankenfeld¹⁰⁸, G.G. Fronze²⁶, U. Fuchs³⁵, C. Furget⁸², A. Furs⁶³, M. Fusco Girard³⁰, J.J. Gaardhøje⁹², M. Gagliardi²⁶, A.M. Gago¹¹³, K. Gajdosova⁹², M. Gallio²⁶, C.D. Galvan¹²², P. Ganoti⁸⁶, C. Garabatos¹⁰⁸, E. Garcia-Solis¹³, K. Garg²⁸, C. Gargiulo³⁵, P. Gasik^{106,36}, E.F. Gauger¹²¹, M.B. Gay Ducati⁷⁴, M. Germain¹¹⁶, J. Ghosh¹¹¹, P. Ghosh¹³⁹, S.K. Ghosh⁴, P. Gianotti⁵¹, P. Giubellino^{35,108,59}, P. Giubilato²⁹, E. Gladzysz-Dziadus¹²⁰, P. Glässel¹⁰⁵, D.M. Gómez Coral⁷⁵, A. Gomez Ramirez⁷⁰, A.S. Gonzalez³⁵, V. Gonzalez¹⁰, P. González-Zamora^{10,2}, S. Gorbunov⁴², L. Görlich¹²⁰, S. Gotovac¹¹⁹, V. Grabski⁷⁵, L.K. Graczykowski¹⁴⁰, K.L. Graham¹¹², L. Greiner⁸³, A. Grelli⁶⁴, C. Grigoras³⁵, V. Grigoriev⁸⁴, A. Grigoryan¹, S. Grigoryan⁷⁸, J.M. Gronefeld¹⁰⁸, F. Grosa³¹, J.F. Grosse-Oetringhaus³⁵, R. Grosso¹⁰⁸, L. Gruber¹¹⁵, F. Guber⁶³, R. Guernane⁸², B. Guerzoni²⁷, K. Gulbrandsen⁹², T. Gunji¹³¹, A. Gupta¹⁰², R. Gupta¹⁰², I.B. Guzman², R. Haake³⁵, C. Hadjidakis⁶², H. Hamagaki⁸⁵, G. Hamar¹⁴², J.C. Hamon¹³⁵, M.R. Haque⁶⁴, J.W. Harris¹⁴³, A. Harton¹³, H. Hassan⁸², D. Hatzifotiadou^{12,54}, S. Hayashi¹³¹, S.T. Heckel⁷¹, E. Hellbär⁷¹, H. Helstrup³⁷, A. Hergelegiu⁸⁸, E.G. Hernandez², G. Herrera Corral¹¹, F. Herrmann⁷², B.A. Hess¹⁰⁴, K.F. Hetland³⁷, H. Hillemanns³⁵, C. Hills¹²⁸, B. Hippolyte¹³⁵, J. Hladky⁶⁷, B. Hohlweger¹⁰⁶, D. Horak³⁹, S. Hornung¹⁰⁸,

R. Hosokawa^{82,132}, P. Hristov³⁵, C. Hughes¹²⁹, T.J. Humanic¹⁸, N. Hussain⁴⁴, T. Hussain¹⁷, D. Hutter⁴², D.S. Hwang²⁰, S.A. Iga Buitron⁷³, R. Ilkaev¹¹⁰, M. Inaba¹³², M. Ippolitov^{84,91}, M. Irfan¹⁷, M.S. Islam¹¹¹, M. Ivanov¹⁰⁸, V. Ivanov⁹⁷, V. Izucheev¹¹⁴, B. Jacak⁸³, N. Jacazio²⁷, P.M. Jacobs⁸³, M.B. Jadhav⁴⁸, J. Jadlovsky¹¹⁸, S. Jaelani⁶⁴, C. Jahnke³⁶, M.J. Jakubowska¹⁴⁰, M.A. Janik¹⁴⁰, P.H.S.Y. Jayarathna¹²⁶, C. Jena⁸⁹, S. Jena¹²⁶, M. Jercic⁹⁹, R.T. Jimenez Bustamante¹⁰⁸, P.G. Jones¹¹², A. Jusko¹¹², P. Kalinak⁶⁶, A. Kalweit³⁵, J.H. Kang¹⁴⁴, V. Kaplin⁸⁴, S. Kar¹³⁹, A. Karasu Uysal⁸¹, O. Karavichev⁶³, T. Karavicheva⁶³, L. Karayan^{108,105}, P. Karczmarczyk³⁵, E. Karpechev⁶³, U. Keschull⁷⁰, R. Keidel¹⁴⁵, D.L.D. Keijdener⁶⁴, M. Keil³⁵, B. Ketzer⁴⁵, Z. Khabanova⁹³, P. Khan¹¹¹, S.A. Khan¹³⁹, A. Khanzadeev⁹⁷, Y. Kharlov¹¹⁴, A. Khatun¹⁷, A. Khuntia⁴⁹, M.M. Kielbowicz¹²⁰, B. Kileng³⁷, B. Kim¹³², D. Kim¹⁴⁴, D.J. Kim¹²⁷, H. Kim¹⁴⁴, J.S. Kim⁴³, J. Kim¹⁰⁵, M. Kim⁶¹, M. Kim¹⁴⁴, S. Kim²⁰, T. Kim¹⁴⁴, S. Kirsch⁴², I. Kisel⁴², S. Kiselev⁶⁵, A. Kisiel¹⁴⁰, G. Kiss¹⁴², J.L. Klay⁶, C. Klein⁷¹, J. Klein³⁵, C. Klein-Bösing⁷², S. Klewin¹⁰⁵, A. Kluge³⁵, M.L. Knichel^{35,105}, A.G. Knospe¹²⁶, C. Kobdaj¹¹⁷, M. Kofarago¹⁴², M.K. Köhler¹⁰⁵, T. Kollegger¹⁰⁸, V. Kondratiev¹³⁸, N. Kondratyeva⁸⁴, E. Kondratyuk¹¹⁴, A. Konevskikh⁶³, M. Konyushikhin¹⁴¹, M. Kopicik¹¹⁸, M. Kour¹⁰², C. Kouzinopoulos³⁵, O. Kovalenko⁸⁷, V. Kovalenko¹³⁸, M. Kowalski¹²⁰, G. Koyithatta Meethalevedu⁴⁸, I. Králík⁶⁶, A. Kravčáková⁴⁰, L. Kreis¹⁰⁸, M. Krivda^{66,112}, F. Krizek⁹⁵, E. Kryshen⁹⁷, M. Krzewicki⁴², A.M. Kubera¹⁸, V. Kučera⁹⁵, C. Kuhn¹³⁵, P.G. Kuijjer⁹³, A. Kumar¹⁰², J. Kumar⁴⁸, L. Kumar¹⁰⁰, S. Kumar⁴⁸, S. Kundu⁸⁹, P. Kurashvili⁸⁷, A. Kurepin⁶³, A.B. Kurepin⁶³, A. Kuryakin¹¹⁰, S. Kushpil⁹⁵, M.J. Kweon⁶¹, Y. Kwon¹⁴⁴, S.L. La Pointe⁴², P. La Rocca²⁸, C. Lagana Fernandes¹²³, Y.S. Lai⁸³, I. Lakomov³⁵, R. Langoy⁴¹, K. Lapidus¹⁴³, C. Lara⁷⁰, A. Lardeux^{76,21}, A. Lattuca²⁶, E. Laudi³⁵, R. Lavicka³⁹, R. Lea²⁵, L. Leardini¹⁰⁵, S. Lee¹⁴⁴, F. Lehas⁹³, S. Lehner¹¹⁵, J. Lehrbach⁴², R.C. Lemmon⁹⁴, V. Lenti⁵³, E. Leogrande⁶⁴, I. León Monzón¹²², P. Lévai¹⁴², X. Li¹⁴, J. Lien⁴¹, R. Lietava¹¹², B. Lim¹⁹, S. Lindal²¹, V. Lindenstruth⁴², S.W. Lindsay¹²⁸, C. Lippmann¹⁰⁸, M.A. Lisa¹⁸, V. Litichevskyi⁴⁶, W.J. Llope¹⁴¹, D.F. Lodato⁶⁴, P.I. Loenne²², V. Loginov⁸⁴, C. Loizides⁸³, P. Loncar¹¹⁹, X. Lopez¹³³, E. López Torres⁹, A. Lowe¹⁴², P. Luettig⁷¹, J.R. Luhder⁷², M. Lunardon²⁹, G. Luparello^{60,25}, M. Lupi³⁵, T.H. Lutz¹⁴³, A. Maevskaya⁶³, M. Mager³⁵, S. Mahajan¹⁰², S.M. Mahmood²¹, A. Maire¹³⁵, R.D. Majka¹⁴³, M. Malaev⁹⁷, L. Malinina^{78,iv}, D. Mal'Kevich⁶⁵, P. Malzacher¹⁰⁸, A. Mamonov¹¹⁰, V. Manko⁹¹, F. Manso¹³³, V. Manzari⁵³, Y. Mao⁷, M. Marchisone^{77,130}, J. Mareš⁶⁷, G.V. Margagliotti²⁵, A. Margotti⁵⁴, J. Margutti⁶⁴, A. Marín¹⁰⁸, C. Markert¹²¹, M. Marquard⁷¹, N.A. Martin¹⁰⁸, P. Martinengo³⁵, J.A.L. Martinez⁷⁰, M.I. Martínez², G. Martínez García¹¹⁶, M. Martinez Pedreira³⁵, S. Masciocchi¹⁰⁸, M. Masera²⁶, A. Masoni⁵⁵, E. Masson¹¹⁶, A. Mastroserio⁵³, A.M. Mathis^{106,36}, P.F.T. Matuoka¹²³, A. Matyja¹²⁹, C. Mayer¹²⁰, J. Mazer¹²⁹, M. Mazzilli³³, M.A. Mazzoni⁵⁸, F. Meddi²³, Y. Melikyan⁸⁴, A. Menchaca-Rocha⁷⁵, E. Meninno³⁰, J. Mercado Pérez¹⁰⁵, M. Meres³⁸, S. Mhlanga¹⁰¹, Y. Miake¹³², M.M. Mieskolainen⁴⁶, D.L. Mihaylov¹⁰⁶, K. Mikhaylov^{65,78}, J. Milosevic²¹, A. Mischke⁶⁴, A.N. Mishra⁴⁹, D. Miśkowiec¹⁰⁸, J. Mitra¹³⁹, C.M. Mitu⁶⁹, N. Mohammadi⁶⁴, B. Mohanty⁸⁹, M. Mohisin Khan^{17,v}, E. Montes¹⁰, D.A. Moreira De Godoy⁷², L.A.P. Moreno², S. Moretto²⁹, A. Morreale¹¹⁶, A. Morsch³⁵, V. Muccifora⁵¹, E. Mudnic¹¹⁹, D. Mühlheim⁷², S. Muhuri¹³⁹, M. Mukherjee⁴, J.D. Mulligan¹⁴³, M.G. Munhoz¹²³, K. Mürning⁴⁵, R.H. Munzer⁷¹, H. Murakami¹³¹, S. Murray⁷⁷, L. Musa³⁵, J. Musinsky⁶⁶, C.J. Myers¹²⁶, J.W. Myrcha¹⁴⁰, D. Nag⁴, B. Naik⁴⁸, R. Nair⁸⁷, B.K. Nandi⁴⁸, R. Nania^{54,12}, E. Nappi⁵³, A. Narayan⁴⁸, M.U. Naru¹⁵, H. Natal da Luz¹²³, C. Nattrass¹²⁹, S.R. Navarro², K. Nayak⁸⁹, R. Nayak⁴⁸, T.K. Nayak¹³⁹, S. Nazarenko¹¹⁰, A. Nedosekin⁶⁵, R.A. Negrao De Oliveira³⁵, L. Nellen⁷³, S.V. Nesbo³⁷, F. Ng¹²⁶, M. Nicassio¹⁰⁸, M. Niculescu⁶⁹, J. Niedziela^{140,35}, B.S. Nielsen⁹², S. Nikolaev⁹¹, S. Nikulin⁹¹, V. Nikulin⁹⁷, F. Noferini^{12,54}, P. Nomokonov⁷⁸, G. Nooren⁶⁴, J.C.C. Noris², J. Norman¹²⁸, A. Nyman⁹¹, J. Nystrand²², H. Oeschler^{19,105,i}, S. Oh¹⁴³, A. Ohlson^{35,105}, T. Okubo⁴⁷, L. Olah¹⁴², J. Olińczak¹⁴⁰, A.C. Oliveira Da Silva¹²³, M.H. Oliver¹⁴³, J. Onderwaater¹⁰⁸, C. Oppedisano⁵⁹, R. Orava⁴⁶, M. Oravec¹¹⁸, A. Ortiz Velasquez⁷³, A. Oskarsson³⁴, J. Otwinowski¹²⁰, K. Oyama⁸⁵, Y. Pachmayer¹⁰⁵, V. Pacik⁹², D. Pagano¹³⁷, P. Pagano³⁰, G. Paic⁷³, P. Palni⁷, J. Pan¹⁴¹, A.K. Pandey⁴⁸, S. Panebianco⁷⁶, V. Papikyan¹, G.S. Pappalardo⁵⁶, P. Pareek⁴⁹, J. Park⁶¹, S. Parmar¹⁰⁰, A. Passfeld⁷², S.P. Pathak¹²⁶, R.N. Patra¹³⁹, B. Paul⁵⁹, H. Pei⁷, T. Peitzmann⁶⁴, X. Peng⁷, L.G. Pereira⁷⁴, H. Pereira Da Costa⁷⁶, D. Peresunko^{91,84}, E. Perez Lezama⁷¹, V. Peskov⁷¹, Y. Pestov⁵, V. Petráček³⁹, V. Petrov¹¹⁴, M. Petrovici⁸⁸, C. Petta²⁸, R.P. Pezzi⁷⁴, S. Piano⁶⁰, M. Pika³⁸, P. Pillot¹¹⁶, L.O.D.L. Pimentel⁹², O. Pinazza^{54,35}, L. Pinsky¹²⁶, D.B. Piyarathna¹²⁶, M. Płoskoń⁸³, M. Planinic⁹⁹, F. Pliquett⁷¹, J. Pluta¹⁴⁰, S. Pochybova¹⁴², P.L.M. Podesta-Lerma¹²², M.G. Poghosyan⁹⁶, B. Polichtchouk¹¹⁴, N. Poljak⁹⁹, W. Poonsawat¹¹⁷, A. Pop⁸⁸, H. Poppenberg⁷², S. Porteboeuf-Houssais¹³³, V. Pozdniakov⁷⁸, S.K. Prasad⁴, R. Preghenella⁵⁴, F. Prino⁵⁹, C.A. Pruneau¹⁴¹, I. Pshenichnov⁶³, M. Puccio²⁶, G. Puudu²⁴, P. Pujahari¹⁴¹, V. Punin¹¹⁰, J. Putschke¹⁴¹, S. Raha⁴, S. Rajput¹⁰², J. Rak¹²⁷, A. Rakotozafindrabe⁷⁶, L. Ramello³², F. Rami¹³⁵, D.B. Rana¹²⁶, R. Raniwala¹⁰³, S. Raniwala¹⁰³, S.S. Räsänen⁴⁶, B.T. Ranganu⁷¹, D. Rathee¹⁰⁰, V. Ratra⁴⁵, I. Ravasenga³¹, K.F. Read^{129,96}, K. Redlich^{87,vi}, A. Rehman²², P. Reichelt⁷¹,

F. Reidt³⁵, X. Ren⁷, R. Renfordt⁷¹, A.R. Reolon⁵¹, A. Reshetin⁶³, K. Reygers¹⁰⁵, V. Riabov⁹⁷, R.A. Ricci⁵², T. Richert³⁴, M. Richter²¹, P. Riedler³⁵, W. Riegler³⁵, F. Riggi²⁸, C. Ristea⁶⁹, M. Rodríguez Cahuantzi², K. Røed²¹, E. Rogochaya⁷⁸, D. Rohr^{35,42}, D. Röhrich²², P.S. Rokita¹⁴⁰, F. Ronchetti⁵¹, E.D. Rosas⁷³, P. Rosnet¹³³, A. Rossi^{29,57}, A. Rotondi¹³⁶, F. Roukoutakis⁸⁶, A. Roy⁴⁹, C. Roy¹³⁵, P. Roy¹¹¹, A.J. Rubio Montero¹⁰, O.V. Rueda⁷³, R. Rui²⁵, B. Rumyantsev⁷⁸, A. Rustamov⁹⁰, E. Ryabinkin⁹¹, Y. Ryabov⁹⁷, A. Rybicki¹²⁰, S. Saarinen⁴⁶, S. Sadhu¹³⁹, S. Sadovsky¹¹⁴, K. Šafařík³⁵, S.K. Saha¹³⁹, B. Sahlmuller⁷¹, B. Sahoo⁴⁸, P. Sahoo⁴⁹, R. Sahoo⁴⁹, S. Sahoo⁶⁸, P.K. Sahu⁶⁸, J. Saini¹³⁹, S. Sakai¹³², M.A. Saleh¹⁴¹, J. Salzwedel¹⁸, S. Sambyal¹⁰², V. Samsonov^{97,84}, A. Sandoval⁷⁵, D. Sarkar¹³⁹, N. Sarkar¹³⁹, P. Sarma⁴⁴, M.H.P. Sas⁶⁴, E. Scapparone⁵⁴, F. Scarlassara²⁹, B. Schaefer⁹⁶, R.P. Scharenberg¹⁰⁷, H.S. Scheid⁷¹, C. Schiaua⁸⁸, R. Schicker¹⁰⁵, C. Schmidt¹⁰⁸, H.R. Schmidt¹⁰⁴, M.O. Schmidt¹⁰⁵, M. Schmidt¹⁰⁴, N.V. Schmidt^{71,96}, J. Schukraft³⁵, Y. Schutz^{135,35}, K. Schwarz¹⁰⁸, K. Schweda¹⁰⁸, G. Scioli²⁷, E. Scomparin⁵⁹, M. Šefčík⁴⁰, J.E. Seger⁹⁸, Y. Sekiguchi¹³¹, D. Sekihata⁴⁷, I. Selyuzhenkov^{108,84}, K. Senosi⁷⁷, S. Senyukov^{3,35,135}, E. Serradilla^{75,10}, P. Sett⁴⁸, A. Sevcenco⁶⁹, A. Shabanov⁶³, A. Shabetaj¹¹⁶, R. Shahoyan³⁵, W. Shaikh¹¹¹, A. Shangaraev¹¹⁴, A. Sharma¹⁰⁰, A. Sharma¹⁰², M. Sharma¹⁰², M. Sharma¹⁰², N. Sharma^{129,100}, A.I. Sheikh¹³⁹, K. Shigaki⁴⁷, Q. Shou⁷, K. Shtejer^{26,9}, Y. Sibiraki⁹¹, S. Siddhanta⁵⁵, K.M. Sielewicz³⁵, T. Siemiarczuk⁸⁷, S. Silaeva⁹¹, D. Silvermyr³⁴, C. Silvestre⁸², G. Simatovic⁹⁹, G. Simonetti³⁵, R. Singaraju¹³⁹, R. Singh⁸⁹, V. Singhal¹³⁹, T. Sinha¹¹¹, B. Sitar³⁸, M. Sitta³², T.B. Skaali²¹, M. Slupecki¹²⁷, N. Smirnov¹⁴³, R.J.M. Snellings⁶⁴, T.W. Snellman¹²⁷, J. Song¹⁹, M. Song¹⁴⁴, F. Soramel²⁹, S. Sorensen¹²⁹, F. Sozzi¹⁰⁸, E. Spiriti⁵¹, I. Sputowska¹²⁰, B.K. Srivastava¹⁰⁷, J. Stachel¹⁰⁵, I. Stan⁶⁹, P. Stankus⁹⁶, E. Stenlund³⁴, D. Stocco¹¹⁶, M.M. Storetvedt³⁷, P. Strmen³⁸, A.A.P. Suaide¹²³, T. Sugitate⁴⁷, C. Suire⁶², M. Suleymanov¹⁵, M. Suljic²⁵, R. Sultanov⁶⁵, M. Šumbera⁹⁵, S. Sumowidagdo⁵⁰, K. Suzuki¹¹⁵, S. Swain⁶⁸, A. Szabo³⁸, I. Szarka³⁸, U. Tabassam¹⁵, J. Takahashi¹²⁴, G.J. Tambave²², N. Tanaka¹³², M. Tarhini⁶², M. Tariq¹⁷, M.G. Tarzila⁸⁸, A. Tauro³⁵, G. Tejada Muñoz², A. Telesca³⁵, K. Terasaki¹³¹, C. Terrevoli²⁹, B. Teyssier¹³⁴, D. Thakur⁴⁹, S. Thakur¹³⁹, D. Thomas¹²¹, F. Thoresen⁹², R. Tieulent¹³⁴, A. Tikhonov⁶³, A.R. Timmins¹²⁶, A. Toia⁷¹, S.R. Torres¹²², S. Tripathy⁴⁹, S. Trogolo²⁶, G. Trombetta³³, L. Tropp⁴⁰, V. Trubnikov³, W.H. Trzaska¹²⁷, B.A. Trzeciak⁶⁴, T. Tsuji¹³¹, A. Tumkin¹¹⁰, R. Turrisi⁵⁷, T.S. Tveter²¹, K. Ullaland²², E.N. Umaka¹²⁶, A. Uras¹³⁴, G.L. Usai²⁴, A. Utrobicic⁹⁹, M. Vala^{118,66}, J. Van Der Maarel⁶⁴, J.W. Van Hoorne³⁵, M. van Leeuwen⁶⁴, T. Vanat⁹⁵, P. Vande Vyvre³⁵, D. Varga¹⁴², A. Vargas², M. Vargyas¹²⁷, R. Varma⁴⁸, M. Vasileiou⁸⁶, A. Vasiliev⁹¹, A. Vauthier⁸², O. Vázquez Doce^{106,36}, V. Vechernin¹³⁸, A.M. Veen⁶⁴, A. Velure²², E. Vercellin²⁶, S. Vergara Limón², R. Vernet⁸, R. Vértesi¹⁴², L. Vickovic¹¹⁹, S. Vigolo⁶⁴, J. Viinikainen¹²⁷, Z. Vilakazi¹³⁰, O. Villalobos Baillie¹¹², A. Villatoro Tello², A. Vinogradov⁹¹, L. Vinogradov¹³⁸, T. Virgili³⁰, V. Vislavicius³⁴, A. Vodopyanov⁷⁸, M.A. Völkl^{105,104}, K. Voloshin⁶⁵, S.A. Voloshin¹⁴¹, G. Volpe³³, B. von Haller³⁵, I. Vorobyev^{106,36}, D. Voscek¹¹⁸, D. Vranic^{35,108}, J. Vrláková⁴⁰, B. Wagner²², H. Wang⁶⁴, M. Wang⁷, D. Watanabe¹³², Y. Watanabe^{131,132}, M. Weber¹¹⁵, S.G. Weber¹⁰⁸, D.F. Weiser¹⁰⁵, S.C. Wenzel³⁵, J.P. Wessels⁷², U. Westerhoff⁷², A.M. Whitehead¹⁰¹, J. Wiechula⁷¹, J. Wikne²¹, G. Wilk⁸⁷, J. Wilkinson^{105,54}, G.A. Willems^{35,72}, M.C.S. Williams⁵⁴, E. Willsher¹¹², B. Windelband¹⁰⁵, W.E. Witt¹²⁹, S. Yalcin⁸¹, K. Yamakawa⁴⁷, P. Yang⁷, S. Yano⁴⁷, Z. Yin⁷, H. Yokoyama^{132,82}, I.-K. Yoo¹⁹, J.H. Yoon⁶¹, V. Yurchenko³, V. Zaccolo⁵⁹, A. Zaman¹⁵, C. Zampolli³⁵, H.J.C. Zanoli¹²³, N. Zardoshti¹¹², A. Zarochentsev¹³⁸, P. Závada⁶⁷, N. Zaviyalov¹¹⁰, H. Zbroszczyk¹⁴⁰, M. Zhalov⁹⁷, H. Zhang^{22,7}, X. Zhang⁷, Y. Zhang⁷, C. Zhang⁶⁴, Z. Zhang^{7,133}, C. Zhao²¹, N. Zhigareva⁶⁵, D. Zhou⁷, Y. Zhou⁹², Z. Zhou²², H. Zhu²², J. Zhu⁷, A. Zichichi^{27,12}, A. Zimmermann¹⁰⁵, M.B. Zimmermann³⁵, G. Zinovjev³, J. Zmeskal¹¹⁵, S. Zou⁷,

Affiliation notes

- ⁱ Deceased
- ⁱⁱ Dipartimento DET del Politecnico di Torino, Turin, Italy
- ⁱⁱⁱ Georgia State University, Atlanta, Georgia, United States
- ^{iv} M.V. Lomonosov Moscow State University, D.V. Skobeltsyn Institute of Nuclear Physics, Moscow, Russia
- ^v Department of Applied Physics, Aligarh Muslim University, Aligarh, India
- ^{vi} Institute of Theoretical Physics, University of Wrocław, Poland

Collaboration Institutes

- ¹ A.I. Alikhanyan National Science Laboratory (Yerevan Physics Institute) Foundation, Yerevan, Armenia
- ² Benemérita Universidad Autónoma de Puebla, Puebla, Mexico
- ³ Bogolyubov Institute for Theoretical Physics, Kiev, Ukraine

- ⁴ Bose Institute, Department of Physics and Centre for Astroparticle Physics and Space Science (CAPSS), Kolkata, India
- ⁵ Budker Institute for Nuclear Physics, Novosibirsk, Russia
- ⁶ California Polytechnic State University, San Luis Obispo, California, United States
- ⁷ Central China Normal University, Wuhan, China
- ⁸ Centre de Calcul de l'IN2P3, Villeurbanne, Lyon, France
- ⁹ Centro de Aplicaciones Tecnológicas y Desarrollo Nuclear (CEADEN), Havana, Cuba
- ¹⁰ Centro de Investigaciones Energéticas Medioambientales y Tecnológicas (CIEMAT), Madrid, Spain
- ¹¹ Centro de Investigación y de Estudios Avanzados (CINVESTAV), Mexico City and Mérida, Mexico
- ¹² Centro Fermi - Museo Storico della Fisica e Centro Studi e Ricerche "Enrico Fermi", Rome, Italy
- ¹³ Chicago State University, Chicago, Illinois, United States
- ¹⁴ China Institute of Atomic Energy, Beijing, China
- ¹⁵ COMSATS Institute of Information Technology (CIIT), Islamabad, Pakistan
- ¹⁶ Departamento de Física de Partículas and IGFAE, Universidad de Santiago de Compostela, Santiago de Compostela, Spain
- ¹⁷ Department of Physics, Aligarh Muslim University, Aligarh, India
- ¹⁸ Department of Physics, Ohio State University, Columbus, Ohio, United States
- ¹⁹ Department of Physics, Pusan National University, Pusan, Republic of Korea
- ²⁰ Department of Physics, Sejong University, Seoul, Republic of Korea
- ²¹ Department of Physics, University of Oslo, Oslo, Norway
- ²² Department of Physics and Technology, University of Bergen, Bergen, Norway
- ²³ Dipartimento di Fisica dell'Università 'La Sapienza' and Sezione INFN, Rome, Italy
- ²⁴ Dipartimento di Fisica dell'Università and Sezione INFN, Cagliari, Italy
- ²⁵ Dipartimento di Fisica dell'Università and Sezione INFN, Trieste, Italy
- ²⁶ Dipartimento di Fisica dell'Università and Sezione INFN, Turin, Italy
- ²⁷ Dipartimento di Fisica e Astronomia dell'Università and Sezione INFN, Bologna, Italy
- ²⁸ Dipartimento di Fisica e Astronomia dell'Università and Sezione INFN, Catania, Italy
- ²⁹ Dipartimento di Fisica e Astronomia dell'Università and Sezione INFN, Padova, Italy
- ³⁰ Dipartimento di Fisica 'E.R. Caianiello' dell'Università and Gruppo Collegato INFN, Salerno, Italy
- ³¹ Dipartimento DISAT del Politecnico and Sezione INFN, Turin, Italy
- ³² Dipartimento di Scienze e Innovazione Tecnologica dell'Università del Piemonte Orientale and INFN Sezione di Torino, Alessandria, Italy
- ³³ Dipartimento Interateneo di Fisica 'M. Merlin' and Sezione INFN, Bari, Italy
- ³⁴ Division of Experimental High Energy Physics, University of Lund, Lund, Sweden
- ³⁵ European Organization for Nuclear Research (CERN), Geneva, Switzerland
- ³⁶ Excellence Cluster Universe, Technische Universität München, Munich, Germany
- ³⁷ Faculty of Engineering, Bergen University College, Bergen, Norway
- ³⁸ Faculty of Mathematics, Physics and Informatics, Comenius University, Bratislava, Slovakia
- ³⁹ Faculty of Nuclear Sciences and Physical Engineering, Czech Technical University in Prague, Prague, Czech Republic
- ⁴⁰ Faculty of Science, P.J. Šafárik University, Košice, Slovakia
- ⁴¹ Faculty of Technology, Buskerud and Vestfold University College, Tonsberg, Norway
- ⁴² Frankfurt Institute for Advanced Studies, Johann Wolfgang Goethe-Universität Frankfurt, Frankfurt, Germany
- ⁴³ Gangneung-Wonju National University, Gangneung, Republic of Korea
- ⁴⁴ Gauhati University, Department of Physics, Guwahati, India
- ⁴⁵ Helmholtz-Institut für Strahlen- und Kernphysik, Rheinische Friedrich-Wilhelms-Universität Bonn, Bonn, Germany
- ⁴⁶ Helsinki Institute of Physics (HIP), Helsinki, Finland
- ⁴⁷ Hiroshima University, Hiroshima, Japan
- ⁴⁸ Indian Institute of Technology Bombay (IIT), Mumbai, India
- ⁴⁹ Indian Institute of Technology Indore, Indore, India
- ⁵⁰ Indonesian Institute of Sciences, Jakarta, Indonesia
- ⁵¹ INFN, Laboratori Nazionali di Frascati, Frascati, Italy
- ⁵² INFN, Laboratori Nazionali di Legnaro, Legnaro, Italy
- ⁵³ INFN, Sezione di Bari, Bari, Italy

- 54 INFN, Sezione di Bologna, Bologna, Italy
- 55 INFN, Sezione di Cagliari, Cagliari, Italy
- 56 INFN, Sezione di Catania, Catania, Italy
- 57 INFN, Sezione di Padova, Padova, Italy
- 58 INFN, Sezione di Roma, Rome, Italy
- 59 INFN, Sezione di Torino, Turin, Italy
- 60 INFN, Sezione di Trieste, Trieste, Italy
- 61 Inha University, Incheon, Republic of Korea
- 62 Institut de Physique Nucléaire d'Orsay (IPNO), Université Paris-Sud, CNRS-IN2P3, Orsay, France
- 63 Institute for Nuclear Research, Academy of Sciences, Moscow, Russia
- 64 Institute for Subatomic Physics of Utrecht University, Utrecht, Netherlands
- 65 Institute for Theoretical and Experimental Physics, Moscow, Russia
- 66 Institute of Experimental Physics, Slovak Academy of Sciences, Košice, Slovakia
- 67 Institute of Physics, Academy of Sciences of the Czech Republic, Prague, Czech Republic
- 68 Institute of Physics, Bhubaneswar, India
- 69 Institute of Space Science (ISS), Bucharest, Romania
- 70 Institut für Informatik, Johann Wolfgang Goethe-Universität Frankfurt, Frankfurt, Germany
- 71 Institut für Kernphysik, Johann Wolfgang Goethe-Universität Frankfurt, Frankfurt, Germany
- 72 Institut für Kernphysik, Westfälische Wilhelms-Universität Münster, Münster, Germany
- 73 Instituto de Ciencias Nucleares, Universidad Nacional Autónoma de México, Mexico City, Mexico
- 74 Instituto de Física, Universidade Federal do Rio Grande do Sul (UFRGS), Porto Alegre, Brazil
- 75 Instituto de Física, Universidad Nacional Autónoma de México, Mexico City, Mexico
- 76 IRFU, CEA, Université Paris-Saclay, Saclay, France
- 77 iThemba LABS, National Research Foundation, Somerset West, South Africa
- 78 Joint Institute for Nuclear Research (JINR), Dubna, Russia
- 79 Konkuk University, Seoul, Republic of Korea
- 80 Korea Institute of Science and Technology Information, Daejeon, Republic of Korea
- 81 KTO Karatay University, Konya, Turkey
- 82 Laboratoire de Physique Subatomique et de Cosmologie, Université Grenoble-Alpes, CNRS-IN2P3, Grenoble, France
- 83 Lawrence Berkeley National Laboratory, Berkeley, California, United States
- 84 Moscow Engineering Physics Institute, Moscow, Russia
- 85 Nagasaki Institute of Applied Science, Nagasaki, Japan
- 86 National and Kapodistrian University of Athens, Physics Department, Athens, Greece
- 87 National Centre for Nuclear Studies, Warsaw, Poland
- 88 National Institute for Physics and Nuclear Engineering, Bucharest, Romania
- 89 National Institute of Science Education and Research, HBNI, Jatni, India
- 90 National Nuclear Research Center, Baku, Azerbaijan
- 91 National Research Centre Kurchatov Institute, Moscow, Russia
- 92 Niels Bohr Institute, University of Copenhagen, Copenhagen, Denmark
- 93 Nikhef, Nationaal instituut voor subatomaire fysica, Amsterdam, Netherlands
- 94 Nuclear Physics Group, STFC Daresbury Laboratory, Daresbury, United Kingdom
- 95 Nuclear Physics Institute, Academy of Sciences of the Czech Republic, Řež u Prahy, Czech Republic
- 96 Oak Ridge National Laboratory, Oak Ridge, Tennessee, United States
- 97 Petersburg Nuclear Physics Institute, Gatchina, Russia
- 98 Physics Department, Creighton University, Omaha, Nebraska, United States
- 99 Physics department, Faculty of science, University of Zagreb, Zagreb, Croatia
- 100 Physics Department, Panjab University, Chandigarh, India
- 101 Physics Department, University of Cape Town, Cape Town, South Africa
- 102 Physics Department, University of Jammu, Jammu, India
- 103 Physics Department, University of Rajasthan, Jaipur, India
- 104 Physikalisches Institut, Eberhard Karls Universität Tübingen, Tübingen, Germany
- 105 Physikalisches Institut, Ruprecht-Karls-Universität Heidelberg, Heidelberg, Germany
- 106 Physik Department, Technische Universität München, Munich, Germany
- 107 Purdue University, West Lafayette, Indiana, United States
- 108 Research Division and ExtreMe Matter Institute EMMI, GSI Helmholtzzentrum für

- Schwerionenforschung GmbH, Darmstadt, Germany
109 Rudjer Bošković Institute, Zagreb, Croatia
110 Russian Federal Nuclear Center (VNIIEF), Sarov, Russia
111 Saha Institute of Nuclear Physics, Kolkata, India
112 School of Physics and Astronomy, University of Birmingham, Birmingham, United Kingdom
113 Sección Física, Departamento de Ciencias, Pontificia Universidad Católica del Perú, Lima, Peru
114 SSC IHEP of NRC Kurchatov institute, Protvino, Russia
115 Stefan Meyer Institut für Subatomare Physik (SMI), Vienna, Austria
116 SUBATECH, IMT Atlantique, Université de Nantes, CNRS-IN2P3, Nantes, France
117 Suranaree University of Technology, Nakhon Ratchasima, Thailand
118 Technical University of Košice, Košice, Slovakia
119 Technical University of Split FESB, Split, Croatia
120 The Henryk Niewodniczanski Institute of Nuclear Physics, Polish Academy of Sciences, Cracow, Poland
121 The University of Texas at Austin, Physics Department, Austin, Texas, United States
122 Universidad Autónoma de Sinaloa, Culiacán, Mexico
123 Universidade de São Paulo (USP), São Paulo, Brazil
124 Universidade Estadual de Campinas (UNICAMP), Campinas, Brazil
125 Universidade Federal do ABC, Santo Andre, Brazil
126 University of Houston, Houston, Texas, United States
127 University of Jyväskylä, Jyväskylä, Finland
128 University of Liverpool, Liverpool, United Kingdom
129 University of Tennessee, Knoxville, Tennessee, United States
130 University of the Witwatersrand, Johannesburg, South Africa
131 University of Tokyo, Tokyo, Japan
132 University of Tsukuba, Tsukuba, Japan
133 Université Clermont Auvergne, CNRS/IN2P3, LPC, Clermont-Ferrand, France
134 Université de Lyon, Université Lyon 1, CNRS/IN2P3, IPN-Lyon, Villeurbanne, Lyon, France
135 Université de Strasbourg, CNRS, IPHC UMR 7178, F-67000 Strasbourg, France, Strasbourg, France
136 Università degli Studi di Pavia, Pavia, Italy
137 Università di Brescia, Brescia, Italy
138 V. Fock Institute for Physics, St. Petersburg State University, St. Petersburg, Russia
139 Variable Energy Cyclotron Centre, Kolkata, India
140 Warsaw University of Technology, Warsaw, Poland
141 Wayne State University, Detroit, Michigan, United States
142 Wigner Research Centre for Physics, Hungarian Academy of Sciences, Budapest, Hungary
143 Yale University, New Haven, Connecticut, United States
144 Yonsei University, Seoul, Republic of Korea
145 Zentrum für Technologietransfer und Telekommunikation (ZTT), Fachhochschule Worms, Worms, Germany